

TRANSIENT PERFORMANCE OF LINEAR INDUCTION LAUNCHERS
 FED BY GENERATORS AND BY CAPACITOR BANKS

J. L. He, Z. Zabar, E. Levi and L. Birenbaum

Polytechnic University
 333 Jay Street, Brooklyn, NY 11201

ABSTRACT

Computer simulation is used to investigate the transient performance of induction-type coilguns as a function of the dimensions, material properties, type of supply, firing sequence of switching elements, and connections of drive coils. The paper deals with the performance of both generator-driven and capacitor-driven coilguns.

1. INTRODUCTION

Coilguns have recently received increased attention because they have important advantages over other electromagnetic launchers. Two of these are absence of contact between the moving and stationary parts, thus permitting repeated use of the barrel, and distribution of the stresses over large surface areas, thus permitting the use of heavier projectiles. Various types of coilguns have been discussed in the literature [1-9]. In comparison with other types of electromagnetic launchers, much more theoretical and experimental work on coilguns remains to be done. This paper deals with the performance analysis of induction-type coilguns. They consist of a projectile with an armature, a barrel with an array of drive coils, and a power supply connected to the barrel drive coils through switches. The barrel of the induction coilgun is usually divided into many sections each of which is operated at a different constant frequency from an independent power supply as shown in Fig. 1. Two of the most commonly used power supplies are generators and capacitor banks. The performance of induction-type coilguns can be very different depending on their power supplies.

Performance of the launcher of Fig. 1 can be described in terms of lumped parameters and a set of matrix equations as shown in [4]. A computer simulation based on these equations was used to obtain the numerical and graphical results presented here.

The generator-driven coilguns are similar to classic linear induction machines. However, they differ from them in the following respects: 1. no ferromagnetic material is used; 2. the secondary (conducting sleeve) is much shorter than the barrel; 3. the transit time of the projectile in the barrel is very short and is comparable to the time constant of the transient electrical currents flowing in the barrel coils and in the sleeve. As a result, the dc component of these currents plays an important role in the launcher performance.

Capacitor-driven coilguns may be classified into two types according to the firing sequence of the switches. The first, called the traveling wave coilgun, is similar to the generator-driven coilgun in many respects. The barrel is divided into many sections. The drive coils in each section are connected in a number of phases, each phase being supplied by a capacitor bank instead of a generator. The capacitance resonates with the inductance of the drive coils, giving rise to (damped)

alternating currents which, as a result of the switching time sequence, build up a traveling wave packet. The other type of capacitor-driven coilgun, called the capacitor-driven multistage coilgun, is the one in which every barrel coil is connected to its own capacitor bank, and the capacitor bank is switched on not according to a pre-programmed time sequence but when the conducting sleeve passes through the middle of the drive coils. In the traveling wave coilgun, one may expect a relatively smooth velocity increase and acceleration. In the capacitor-driven multistage coilgun, on the other hand, there exist strong force fluctuations, even when the average acceleration is small.

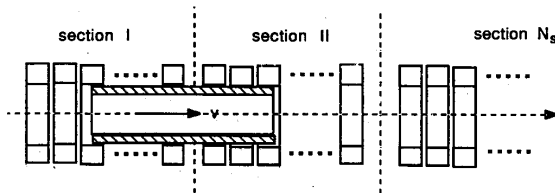


Fig. 1 Sketch of multisection induction coil launcher

2. PERFORMANCE OF A GENERATOR-DRIVEN
 COILGUN

Starting Section

The specific computer simulation model to be studied here assumes that the starting section of the generator-driven coilgun consists of 6 drive coils connected in a three phase arrangement; i.e. the six drive coils have the phase sequence A, -C, B, -A, C, -B. A 100-gram aluminum sleeve is used as the projectile. Detailed dimensions are given in Table 1 below. If one neglects the generator internal impedance, the three phase voltages may be considered constant so that:

$$V_a = V_m \cos(\omega t + \phi) \quad (1)$$

$$V_b = V_m \cos(\omega t - 120^\circ + \phi) \quad (2)$$

$$V_c = V_m \cos(\omega t - 240^\circ + \phi) \quad (3)$$

where the radian frequency $\omega = 2\pi f$ and the pole pitch τ are related to the synchronous velocity v_s by $v_s = 2\tau f$, and ϕ , the switch-on phase angle, depends on the instant at which the generator is switched on. It is noted that during the transients, and because of the finite length of the driver sections and of the armature, there exists a continuous spectrum of wavelengths and frequencies.

"Synchronous velocity" is used here to refer only to the fundamental components in space and time. As a result of these higher harmonics, the currents induced in the sleeve and therefore the forces do not vanish at synchronous velocity.

A 2000 V peak voltage and 1250 Hz constant frequency is applied to the barrel. The three phase currents are shown in Fig. 2. It is seen that these currents are asymmetrical because of dc components, especially in phases B and C, during the first millisecond. Because of this asymmetry, the muzzle velocity of the projectile in the starting section varies slightly with the switching-on time; i.e. it varies with the switch-on phase ϕ in Eqs. (1)-(3). This is shown in Fig. 3, from which one can see that the muzzle velocity changes by about 10% as the switch-on phase varies from 0° to 360° . This implies that since the switch-on time of the generators is arbitrary, and may be any instant of time within a complete period, the performance would not be expected to be repetitive. The velocity and acceleration profiles are smooth, as shown in Fig. 4. This means that in the starting section, the dc components affect only the initial acceleration.

The initial projectile position in the starting section is also an important factor that affects the muzzle velocity. The best initial position for the sleeve is around the position where the left end of the sleeve is aligned with the left end of the barrel. The sleeve conductivity also affects the starting performance. It is seen from Fig. 5 that there exists an optimum conductivity for specified coilgun dimensions. It is not correct to assume that the higher the conductivity, the better is the performance, or the higher is the muzzle velocity. Figure 5 shows that for the dimensions in this example the best value of the conductivity is around 2.4×10^7 S/m. According to conventional electrical machinery theory, the induction force depends on the slip between the wave velocity and sleeve velocity, and there exists a peak value at critical slip. Since different conductivity leads to a different critical slip, and to a different value at which the maximum force occurs, the profile of the force acting on the sleeve during the transit time in the barrel also changes.

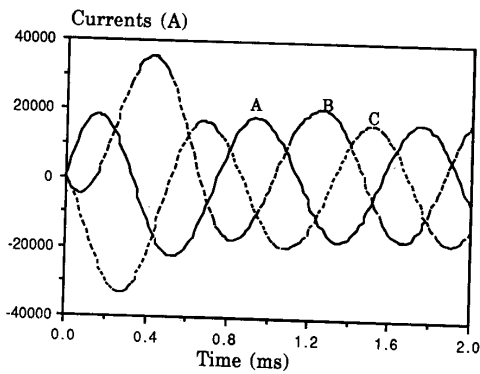


Fig. 2 Three phase currents in the starting section. $V_m=2000$ V, $f=1250$ Hz

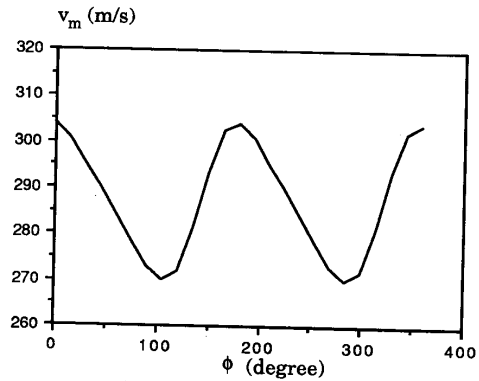


Fig.3 Dependence of muzzle velocity on switching-on phase angles ϕ . $V_m=2000$ V, $f=1250$ Hz.

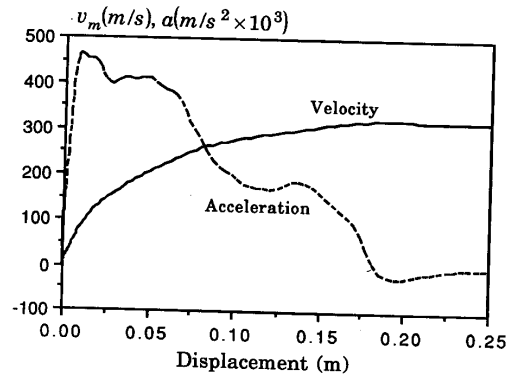


Fig. 4 Velocity and acceleration profiles of generator-driven coilgun in the starting section. $V_m=2000$ V, $f=1250$ Hz.

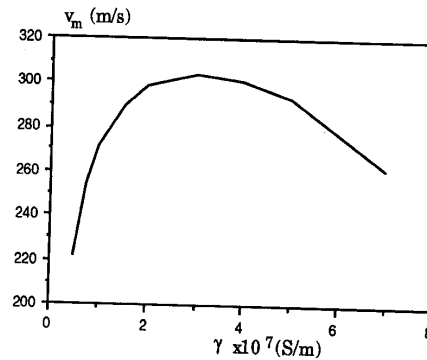


Fig. 5 Dependence of muzzle velocity on sleeve conductivity. $V_m=2000$ V, $f=1250$ Hz, $\phi=0^\circ$.

Effect of the dc components of current at high velocity

At high velocity, the transit time of the projectile in the barrel is of the same order as the electrical transient time constant, so that the dc components of current in the barrel coils can produce a large retarding force which is comparable to the propulsive force. Thus, at higher velocity, the acceleration may become negative.

Simulations were made for a 40 cm length of barrel with 12 drive coils connected into three phase windings. The following assumptions were made: peak voltage - 35 kV; frequency - 5000 Hz; initial projectile velocity - 800 m/s; initial sleeve current - zero. The assumption of zero initial sleeve current makes it possible to separate the effects on performance due to transition between the two sections from that due to the effect of the dc components of current. The other dimensions are the same as before. The muzzle velocity was found to be 1003 m/s.

It is seen from Fig. 6 that the three phase currents in the barrel include strong dc components, especially, in phases B and C. As shown in Fig. 7, the acceleration profile is divided into two regions: in the first half section, the projectile is subjected to a braking force; only in the last half section is the projectile accelerated. This implies that at high velocity the dc components in the three phase currents destroy the traveling wave. In other words, the coilgun would not be able to operate at a velocity higher than 1000 m/s unless special measures were adopted.

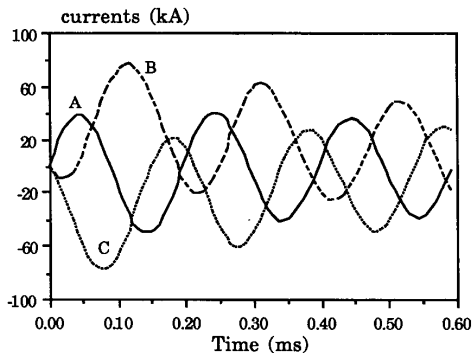


Fig. 6 Three phase currents in the barrel coils. $V_m=35$ kV, $f=5000$ Hz and $v_m=1003$ m/s muzzle velocity.

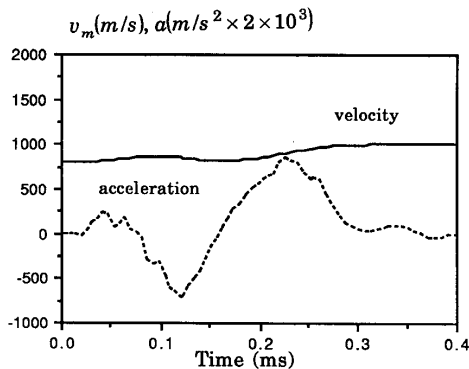


Fig. 7 Velocity and acceleration profiles in the high velocity section. $v_m=1003$ m/s, $V_m=35$ kV and $f=5000$ Hz.

One way to eliminate this problem is to switch on the three phase voltages in sequence. The instant of time in which each phase voltage is switched on would be determined by checking the zero current crossing point in each phase. Since the currents in the barrel coils are determined by the load, this would necessitate a pre-estimate of the current and the power factor in each phase.

Transition between sections

The transition of the projectile from a lower velocity section to a higher velocity one is a major factor in determining the feasibility of achieving hyper-velocity in the induction coilgun. The simulation here is based on a model that has two sections: a starting section, and a second one with 12 drive coils. The frequencies and the voltages are 1250 Hz, 2000 V peak; and 2500 Hz, 6000 V peak in each section respectively. The sleeve enters the second section with the current induced in the first section. The power supply in the second section is switched on at different time instants and at different positions of the sleeve in the second section.

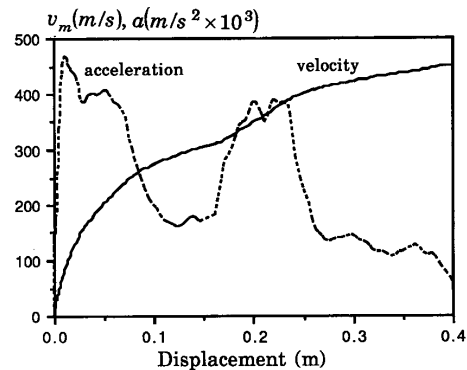


Fig. 8 Velocity and acceleration profiles in a two-section barrel. $\phi=0$

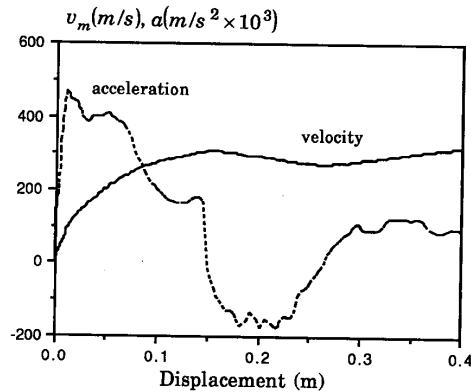


Fig. 9 Velocity and acceleration profiles in a two-section barrel. $\phi=100^\circ$

The results show that two major problems are involved in the transition process: one is the current phase difference between the sleeve current induced in the previous section and in the present section and other one is the dc component effect mentioned before. The first problem could be solved by switching on the power supply in the second section when more than half of the sleeve has entered the second section. In this case, the sleeve current induced in the previous section has had time to decay. Thus the "braking", or negative acceleration may be avoided even if the two currents still have different phase angles. This problem will be aggravated at high velocities because of the short transition time. However, the second problem, the asymmetrical current effect, still plays an important role. This can be seen from Figs. 8 and 9. In both, the second section was energized simultaneously in all phases when three quarters of the sleeve length was already in. It is seen from Fig. 8 that a smooth transition is achieved at zero switch-on phase angle, i.e. $\phi=0^\circ$. However, almost complete braking appears at $\phi=100^\circ$ as shown in Fig. 9. A comparison of Figs. 3 and 9 shows that small dc components do not seriously affect the performance at starting, but play a significant role at the transition between the sections. It follows that since energization of the next section cannot be made to occur always at the most propitious moment, the dc component must be eliminated by switching on the power supplies phase by phase in order to obtain a smooth transition between the sections.

3. PERFORMANCE OF CAPACITOR-DRIVEN TRAVELING WAVE COILGUN [4]

The starting section of the barrel is assumed to be the same as in the generator-driven coilgun, i.e. there are six drive coils on the barrel connected in a three phase arrangement with phase sequence A, -C, B, -A, C, -B. However, three capacitor banks each with capacitance $1500 \mu\text{F}$, replace the three generator sources. As was already mentioned the traveling wave is built up by the resonance between the capacitance and the inductance of the drive coils, and by firing the three capacitor banks in sequence at different phase angles so as to produce a "three phase system". The value of capacitance was determined by matching the resonant frequency to the "synchronous" frequency. Computer simulations show that the performance of the gun depends on many factors, such as initial position, firing phase shift, total barrel coil resistance and sleeve

conductivity. The dimensions given in Table 1 were also used in this simulation for comparison. Capacitors were initially charged up to 3500, 3000, and 2500 V in each phase respectively. The different voltage levels are required to make up for the different attenuations in each phase due to the firing time sequence. The three phase capacitor banks were fired in sequence: first phase A; then phase C after 60° with negative initial capacitor voltage; and last, phase B after another 60° . Figure 10 shows the three phase capacitor discharge currents. It is seen that these currents are strongly attenuated. The reason for this high attenuation is that at lower velocity, or at starting, the projectile armature (sleeve) dissipates a lot of energy. Besides, the attenuation is also caused by the resistance of the barrel coils, the switches and the leads. This is the main reason why the capacitor-driven coilgun may need a

relatively higher voltage when compared with the generator-driven coilgun. Velocity and acceleration profiles for the starting section are shown in Fig. 11 from which one can see that the acceleration is relatively smooth and the velocity builds up within a short distance. It follows from the attenuation that the length of a section in a capacitor-driven coilgun should be limited to a few wave lengths.

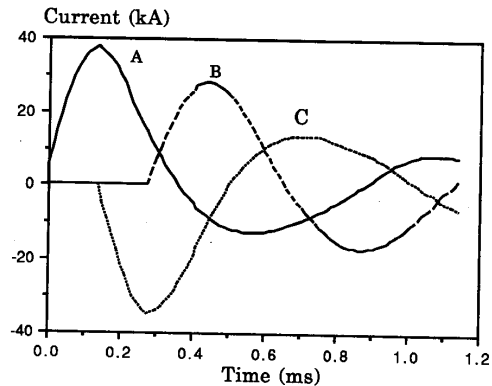


Fig. 10 Three phase currents in the starting section. $V_c = 3500, 3000, 2500 \text{ V}$ and $C = 1500 \mu\text{F}/\text{phase}$.

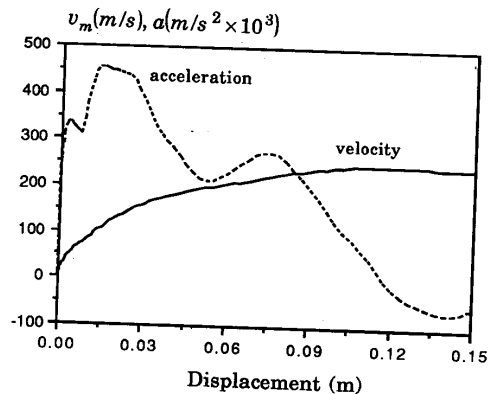


Fig. 11 Velocity and acceleration profiles in the starting section. $V_c = 3500, 3000, 2500 \text{ V}$ for the three phases, and $C = 1500 \mu\text{F}/\text{phase}$.

The starting performance also strongly depends on the initial sleeve position. Similarly to the generator-driven coilgun, the best initial sleeve position is around the position where the left end of the sleeve is aligned with the left end of the barrel, or is a few millimeters inside the barrel, as shown in Fig. 12. It is seen from Fig. 12 that the muzzle velocity decreases sharply when the initial position of the sleeve is moved to the left, but is not very sensitive to a displacement to the right.

The firing sequence of the capacitor banks in each phase determines the phase shifts among the three phases. They are a key factor in building a traveling wave. It is interesting to observe from Fig. 13 that for specified total input energy, the highest muzzle velocity is achieved with a sixty-degree phase shift between phases.

Unlike the generator-driven coilgun, the performance of a capacitor-driven coilgun is very sensitive to the total resistance of the drive coils. Figure 14 shows the dependence of muzzle velocity on the total resistance per drive coil. One can see that muzzle velocity drops sharply as the resistance increases. To have a better performance, one should keep the total barrel resistance as small as possible. The effect of sleeve conductivity on the muzzle velocities is given in Fig. 15. There exists an optimum value of conductivity which gives the highest muzzle velocity for specified coilgun dimensions and input energy. It is interesting to find out that the shapes of Fig. 5 and Fig. 15 are similar.

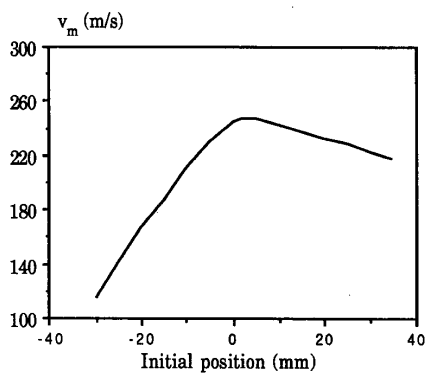


Fig. 12 Dependence of muzzle velocity on initial sleeve position. Zero represents the position where left end of the sleeve is aligned with the left end of the barrel.

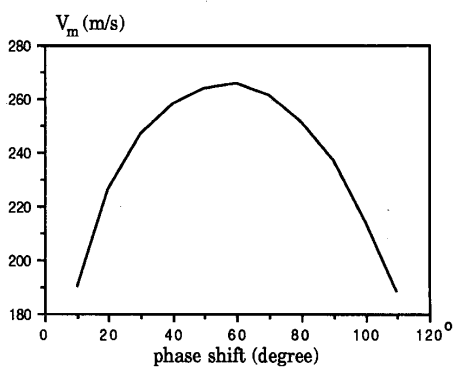


Fig. 13 Dependence of muzzle velocity on firing sequence, or phase shift. $V_c=3500, 3000,$ and 2500 V per phase respectively. $C=1500 \mu\text{F/phase}$.

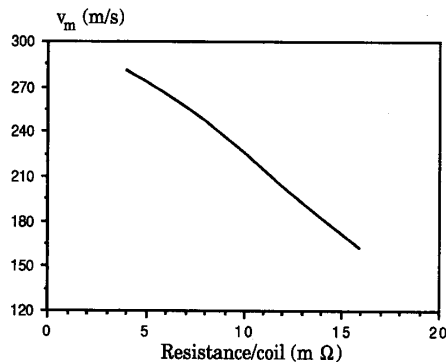


Fig. 14 Dependence of muzzle velocity of first section on the total resistance per drive coil. $V_c=3500, 3000,$ and 2500 V per phase respectively. $C=1500 \mu\text{F/phase}$.

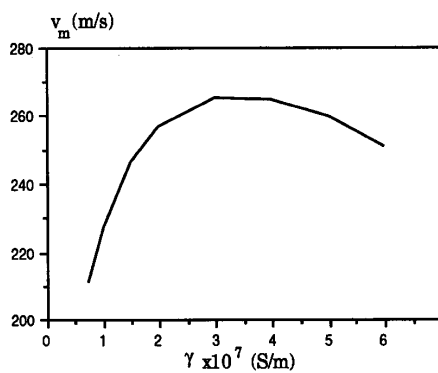


Fig. 15 Dependence of muzzle velocity in the first section on conductivity of the sleeve. $V_c=3500, 3000,$ and 2500 V respectively. $C=1500 \mu\text{F/phase}$.

The performance of the capacitor-driven coilgun at high velocity (up to 1000 m/s) was discussed in reference [4]. The problems regarding the transition between the sections were discussed in references [4] and [9].

Table 1 DIMENSIONS FOR SIMULATION MODEL

Starting Section:	
Length ($=2\tau$)	20 cm
Number of coils	6 (10 turns/coil)
Radial thickness of coil	1.5 cm
Axial length of coil	3 cm
Average radius	3.425 cm

Higher Velocity Section:

It has the same cross section as the starting section but double the length and number of drive coils.

Sleeve Dimensions:

Length	20 cm
Average radius	2.5 cm
Radial thickness	1.3 mm
Material	aluminum
Weight	100 g
Clearance between sleeve and barrel coils	1 mm

CONCLUDING REMARKS

The generator-driven coilgun performs satisfactorily in the starting section. However, at high velocity, the transit time is close to the electrical transient time constant, and therefore the dc components produce a retarding force. To avoid this problem, the three phase voltages should not be switched on simultaneously, but rather phase by phase according to their zero current crossing points. This can also alleviate the problem in the transition between the sections. The capacitor-driven coilguns, instead, derive the alternating current needed to create a traveling wave from resonance with the inductance of the coils. Therefore, the initiation of the sinusoidal current oscillation coincides with the switch-on time. They are ideally suited for short-time, high acceleration operation, but they are likely to require higher operating voltages than the generator-driven coilguns, because of the constraint imposed on the capacitance by the resonance condition with attenuation. In general, it is difficult to achieve a smooth transition between one section and the next. However, it is possible for both coilguns to avoid negative acceleration by turning on the source phase by phase at a certain instant of time. Further theoretical analysis and high velocity tests should be made on both coilguns.

ACKNOWLEDGEMENT

This work was sponsored by the SDIO/IST and managed by USASDC under contract No. DASG60-88-C-0047.

REFERENCES

1. T. J. Burgess, E. C. Cnare, W. L. Oberkamp, S. G. Beard and M. Cowan, "The Electromagnetic θ Gun and Tubular Projectiles", IEEE Transactions on Magnetism, Vol. MAG-18, No. 1, Jan. 1982 pp. 46-59.
2. P. Mongeau and F. Williams, "Arc-Commutated Launcher," IEEE Transactions on Magnetism, Vol. MAG-18, No. 1, Jan. 1982, pp. 42-45.
3. M. D. Driga, W. F. Weldon, and H. H. Woodson, "Electromagnetic Induction Launchers," IEEE Transactions on Magnetism, Vol. MAG-22, No. 6, Nov. 1986 pp. 1453-1458.
4. J. L. He, E. Levi, Z. Zabar, and L. Birenbaum, "Concerning the Design of Capacitively-Driven Induction Coil-Guns," IEEE Transactions on Plasma Science, June 1989, Vol. 17, No. 3, pp. 429-438.
5. M. Cowan, E. C. Cnare, B. W. Duggin, R. J. Kaye and T. J. Tucker, "The Reconnection Gun," IEEE Transactions on Magnetism, Vol. 22, No. 6, Nov. 1986, pp. 1429-1434.
6. D. G. Elliott, "Traveling-Wave Inductive Launchers", IEEE Transactions on Magnetism, Vol. 25, No. 1, Jan. 1989, pp. 159-163.
7. P. Mongeau, W. Snow, G. Colello, P. Rezza and H. Kolm, "Coilgun Technology Evolution", 4th Symposium on Electromagnetic Launcher Technology, Austin, Texas, April 12-14, 1988.
8. D. G. Elliott, "Study of Advanced Electromagnetic Launchers," Progress Report No. 5, JPL, California Institute of Technology, JPL D-5413, May 13 1988.
9. Z. Zabar et al, "Test Results for Three Prototype Models of a Linear Induction Launcher", 5th Electromagnetic Launcher Symposium, Sandestin, Florida, April 2-5, 1990.